

Probability of collision between a rectangular cuboid and small debris

Ricardo García-Pelayo and Juan Luis Gonzalo

Abstract The probability of collision between a rectangular cuboid and small debris (that is, point-like debris) is computed, under the assumptions of the short-encounter model. The computation is exact in the sense that it is not based on approximations such as the enveloping sphere approximation, but on a very efficient algorithm to compute the integral of Gaussian over the projection of a rectangular cuboid on the collision plane.

1 Introduction

Estimating the probability of collision between orbiting objects is a fundamental task in space security awareness. The probability of collision needs to be computed whenever an active spacecraft experiences a critical conjunction in order to determine whether or not a propulsive collision avoidance maneuver should be performed. Lastly, if a maneuver is eventually required it can only be optimized with the aid of a proper collision probability estimation method [3].

There is an abundant literature dealing with the computation of the collision probability when the two approaching bodies are spheres [8, 12, 5, 2, 14, 10]. Of these, the methods [14, 10] are the most computationally efficient. Method [10] is the only one that can be applied to the non-Gaussian case.

The spherical envelope of the true spacecraft geometry provides a good conservative bound of the collision probability for the case of, say, two satellites. But it may grossly overestimate the probability when at least one of the two objects is far

Ricardo García-Pelayo
ETS de Ingeniería Aeronáutica y del Espacio (UPM), Pza. del Cardenal Cisneros 3, Madrid 28040,
Spain, e-mail: r.garcia-pelayo@upm.es

Juan Luis Gonzalo
Politecnico di Milano, Department of Aerospace Science and Technology, via Giuseppe La Masa
34, Milan 20156, Italy, e-mail: juanluis.gonzalo@polimi.it

from spherical. In particular when the spacecraft has the shape of a cube, the area of its projection onto a plane is at most $\sqrt{3} = 1.732\dots$, while the projection of its enveloping sphere is a circle of area $3\pi/4 = 2.356\dots$. Thus the spherical envelope approximation to a rectangular cuboid overestimates the area of its projection onto the collision plane by at least 36%. The error of the input in this field are large, especially due to the probability density function of the relative position. However, one should try that the methods of computation do not introduce further errors larger than 10%.

In this paper we compute the probability of collision between a spacecraft in the shape of a rectangular cuboid and a piece of debris of negligible size under the assumptions of short-encounter model [8, 1, 12, 2, 5, 6, 3, 14]. These are: the projection ρ of the probability density function (henceforth, pdf) of the relative position of the spacecraft and the debris at the moment of conjunction is known and so is the direction of the relative velocity at that moment. ρ can be found from the pdf's of the positions P and Q , ρ_P and ρ_Q [9] (see Fig. 1). The direction of the relative velocity needs to be known so that the collision plane, which is perpendicular to it, is well defined. A typical use of this probability of collision is to decide if an evasive maneuver will be made or not.

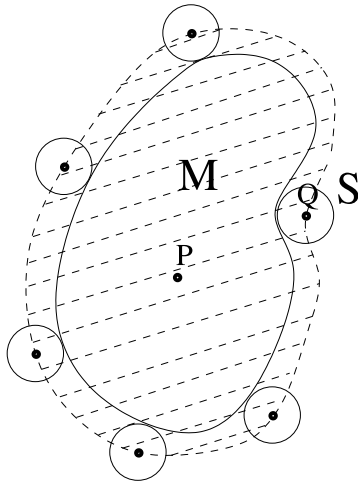


Fig. 1 The collision region in the encounter plane is found by sliding the projection of the debris or the satellite (the circle S) around the projection M .

First we give an overview of how the probability of collision would be computed if the debris were not of negligible size compared to the spacecraft, so that the approximation done in this paper becomes clear. Suppose that M in Fig. 1 were the projection of the spacecraft onto the collision plane. Then there would be collision if and only if the vector \mathbf{PQ} lies inside the shaded area. The shaded area is called the Minkowski sum of M and the projection of the debris, which is the disk with center

Q shown in the Figure. This is explained with greater generality in [9]. Then in the general case the probability of collision is

$$\int_{M \oplus (-S)} d^2r \rho(\mathbf{r}), \quad (1)$$

where $M \oplus (-S)$ denotes the shaded region in Fig. 1 [9] and $\rho(\mathbf{r})$ is the pdf of the relative position. When the debris is of negligible size then the rim of M in 1 disappears and we just need to compute the integral over the projection M . When the spacecraft is a rectangular cuboid (or a parallelepiped) the projection is a hexagon which is made up of three disjoint parallelograms. $\rho(\mathbf{r})$ is almost always taken to be a Gaussian. Recently a very efficient algorithm was implemented to compute precisely that integral [9], which was based on a previous work of Genz. There is web app (together with its source code) at <http://sdg.aero.upm.es/index.php/online-apps/gaussian-over-parallelogram> where such integral can be computed.

2 Projection of the rectangular cuboid

Let a, b and c be the lengths of the sides of the rectangular cuboid. We choose a Cartesian coordinate frame in which the z axis is parallel to the relative velocity between the cuboid and the debris and points towards the cuboid. The x axis has the direction of projection of the side of length a and the y axis completes a right-handed frame. Let P denote the vertex which is expected to cross the collision plane first. Then the angles θ_a, θ_b and θ_c made by the three sides which meet at P and the z axis satisfy $0 \leq \theta_a, \theta_b, \theta_c \leq \pi/2$. θ_c is determined by the other three angles, therefore we shall give the formulae in terms of θ_a and θ_b only. In a generic position of the cuboid the three faces meeting at vertex P yield a projection on the collision plane, and this is the case that we shall consider here. In non generic cases only two or one faces project onto the collision plane.

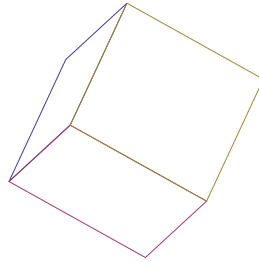


Fig. 2 Flat projection of a cube in a generic position.

Each of the three faces of the cuboid is a rectangle and the projection of a rectangle onto a plane is a parallelogram. Indeed, a projection is a linear transformation

(see, e. g., [4], p. 113) and thus it transforms parallel lines into parallel lines. As an example, the projection of a cube is shown in Fig. 2

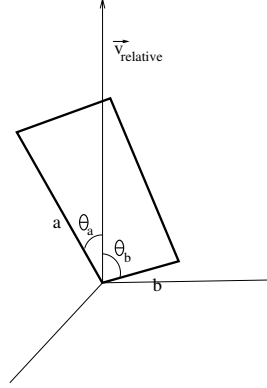


Fig. 3 Angles θ_a and θ_b are shown.

We define spherical coordinates where θ is the colatitude (angle made with the positive direction of the z -axis) and φ is the longitude. The coordinates of the unit vectors associated with the sides of lengths a and b are $\mathbf{u}_a = (\sin \theta_a \cos \varphi_a, \sin \theta_a \sin \varphi_a, \cos \theta_a)$ and $\mathbf{u}_b = (\sin \theta_b \cos \varphi_b, \sin \theta_b \sin \varphi_b, \cos \theta_b)$ (see Fig. 3). The cosine of the angle θ_c is the third component of $\mathbf{u}_a \times \mathbf{u}_b$, which is

$$\cos \theta_c = \sin(\varphi_b - \varphi_a) \sin \theta_a \sin \theta_b. \quad (2)$$

Since \mathbf{u}_a and \mathbf{u}_b are perpendicular, $\mathbf{u}_a \cdot \mathbf{u}_b = \cos \theta_a \cos \theta_b + \sin \theta_a \sin \theta_b \cos(\varphi_b - \varphi_a) = 0 \Rightarrow$

$$\cos(\varphi_b - \varphi_a) = -\frac{\cos \theta_a \cos \theta_b}{\sin \theta_a \sin \theta_b}. \quad (3)$$

Since $0 \leq \theta_a, \theta_b \leq \pi/2$, the four trigonometrical functions that appear in the rhs of eq. (3) are positive and $\pi/2 \leq |\varphi_b - \varphi_a| \leq \pi$. Furthermore, $\cos(\theta_a + \theta_b) = -(\sin \theta_a \sin \theta_b - \cos \theta_a \cos \theta_b) \leq 0 \Rightarrow \pi/2 \leq \theta_a + \theta_b \leq \pi$. Thus, when θ_a and θ_b are both between 0 and $\pi/2$ and θ_a is given, $(\pi/2) - \theta \leq \theta_b \leq \pi - \theta$. This can be used as a test to reject invalid input data when writing a program.

Equation (3) allows us to write \mathbf{u}_a , \mathbf{u}_b and \mathbf{u}_c in terms of θ_a , θ_b and φ_a only:

$$\begin{aligned} \mathbf{u}_b = & (\sin \theta_b \cos(\varphi_a + (\varphi_b - \varphi_a)), \sin \theta_b \sin(\varphi_a + (\varphi_b - \varphi_a)), \cos \theta_b) = \\ & \left(-\sin \theta_b \left(\cos \varphi_a \frac{\cos \theta_a \cos \theta_b}{\sin \theta_a \sin \theta_b} + \sin \varphi_a \frac{\sqrt{-\cos(\theta_a + \theta_b) \cos(\theta_a - \theta_b)}}{\sin \theta_a \sin \theta_b} \right), \right. \end{aligned}$$

$$\begin{aligned} & \sin \theta_b \left(-\sin \varphi_a \frac{\cos \theta_a \cos \theta_b}{\sin \theta_a \sin \theta_b} + \cos \varphi_a \frac{\sqrt{-\cos(\theta_a + \theta_b) \cos(\theta_a - \theta_b)}}{\sin \theta_a \sin \theta_b} \right), \cos \theta_b \Big) = \\ & \frac{1}{\sin \theta_a} \left(-\cos \varphi_a \cos \theta_a \cos \theta_b - \sin \varphi_a \sqrt{-\cos(\theta_a + \theta_b) \cos(\theta_a - \theta_b)}, \right. \\ & \left. -\sin \varphi_a \cos \theta_a \cos \theta_b + \cos \varphi_a \sqrt{-\cos(\theta_a + \theta_b) \cos(\theta_a - \theta_b)}, \sin \theta_a \cos \theta_b \right). \quad (4) \end{aligned}$$

$$\mathbf{u}_c = \mathbf{u}_a \wedge \mathbf{u}_b =$$

$$\begin{aligned} & \left(\frac{-\cos \varphi_a \sqrt{-\cos(\theta_a - \theta_b) \cos(\theta_a + \theta_b)} \cos \theta_a + \cos \theta_b \sin \varphi_a}{\sin \theta_a}, \right. \\ & \left. \frac{-\cos \varphi_a \cos \theta_b - \sqrt{-\cos(\theta_a - \theta_b) \cos(\theta_a + \theta_b)} \cos \theta_a \sin \varphi_a}{\sin \theta_a}, \right. \\ & \left. \sqrt{-\frac{\cos 2\theta_a + \cos 2\theta_b}{2}} \right). \quad (5) \end{aligned}$$

The choice $\varphi = 0$ simplifies the preceding expressions to:

$$\mathbf{u}_a = (\sin \theta_a, 0, \cos \theta_a) \quad (6)$$

$$\mathbf{u}_b = \frac{1}{\sin \theta_a} \left(-\cos \theta_a \cos \theta_b, \sqrt{-\cos(\theta_a + \theta_b) \cos(\theta_a - \theta_b)}, \sin \theta_a \cos \theta_b \right). \quad (7)$$

$$\mathbf{u}_c =$$

$$\left(\frac{-\sqrt{-\cos(\theta_a - \theta_b) \cos(\theta_a + \theta_b)} \cos \theta_a}{\sin \theta_a}, \frac{-\cos \varphi_a \cos \theta_b}{\sin \theta_a}, \sqrt{-\frac{\cos 2\theta_a + \cos 2\theta_b}{2}} \right). \quad (8)$$

We define the vectors

$$\left. \begin{aligned} \mathbf{a} &= a \mathbf{u}_a \\ \mathbf{b} &= b \mathbf{u}_b \\ \mathbf{c} &= c \mathbf{u}_c \end{aligned} \right\} \quad (9)$$

and their projections \mathbf{a}' , \mathbf{b}' , \mathbf{c}' on the xy plane (see Fig. 4), which are

$$\mathbf{a}' = a(\sin \theta_a, 0, 0), \quad (10)$$

$$\mathbf{b}' = \frac{b}{\sin \theta_a} \left(-\cos \theta_a \cos \theta_b, \sqrt{-\cos(\theta_a + \theta_b) \cos(\theta_a - \theta_b)}, 0 \right), \quad (11)$$

$$\mathbf{c}' = c \left(\frac{-\sqrt{-\cos(\theta_a - \theta_b) \cos(\theta_a + \theta_b)} \cos \theta_a}{\sin \theta_a}, \frac{-\cos \theta_a \cos \theta_b}{\sin \theta_a}, 0 \right). \quad (12)$$

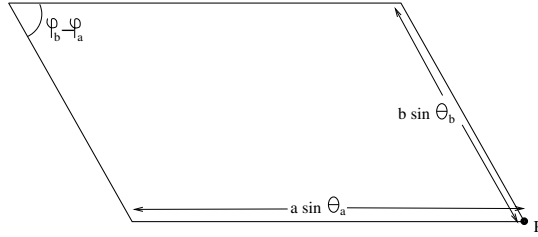


Fig. 4 Projection of the face of sides a and b onto the collision plane.

The area of the projected hexagon is

$$|\mathbf{a}' \wedge \mathbf{b}'| + |\mathbf{b}' \wedge \mathbf{c}'| + |\mathbf{c}' \wedge \mathbf{a}'| = ab \sqrt{\frac{\cos 2\theta_a + \cos 2\theta_b}{2}} + bc |\cos \theta_a| + ca |\cos \theta_b|. \quad (13)$$

The four corners of each of the parallelograms are

$$\left. \begin{array}{l} \mathbf{OP} + \frac{\pm \mathbf{a}' \pm \mathbf{b}'}{2} \\ \mathbf{OP} + \frac{\pm \mathbf{b}' \pm \mathbf{c}'}{2} \\ \mathbf{OP} + \frac{\pm \mathbf{c}' \pm \mathbf{a}'}{2} \end{array} \right\}. \quad (14)$$

3 Computation of the probability of collision

We are going to suppose that ρ_{rel} is a Gaussian, because the pdf's of the position, in terms of which ρ_{rel} is defined, are almost always given as Gaussians. The enclosing parallelogram are now completely determined. The problem at hand is to evaluate the integral

$$\frac{1}{2\pi \det \Sigma} \int_{Par} dx dy \exp -\frac{1}{2} (x, y) \cdot \Sigma^{-1} \cdot \begin{pmatrix} x \\ y \end{pmatrix}, \quad (15)$$

over each of the parallelograms, where Σ is the covariance matrix,

$$\Sigma = \begin{pmatrix} \sigma_x^2 & \sigma_{xy} \\ \sigma_{xy} & \sigma_y^2 \end{pmatrix}. \quad (16)$$

In order to do this integral we shall develop a method for the computation of bivariate normal probabilities in rectangular domains based on the work of Genz [11].

In [11] Genz proposed and compared several algorithms for the numerical computation of bivariate, trivariate normal distribution and Student t probability distributions. In particular, a very fast algorithm was presented to compute the bivariate normal probability $L(h, k, \rho)$ for a domain of the form $[h, \infty) \times [k, \infty)$ ($h, k \in \Re$) and a Gaussian of correlation $\rho \in [0, 1]$ and $\sigma_x = \sigma_y = 1$. Note that L is related to the standard bivariate normal cumulative distribution Φ by the expression $\Phi((x, y), \rho) = L(-x, -y, \rho)$. A more detailed description of the algorithm can be found in the Appendix.

We are going to explain the procedure for the parallelogram whose sides are the vectors $\mathbf{a}' = (a'_x, a'_y, 0)$ and $\mathbf{b}' = (b'_x, b'_y, 0)$. It is always possible to find a linear transformation M that transforms the parallelogram into a square of unit side by imposing:

$$M\mathbf{a}' = \begin{pmatrix} 1 \\ 0 \end{pmatrix}, \quad M\mathbf{b}' = \begin{pmatrix} 0 \\ 1 \end{pmatrix}. \quad (17)$$

Combining these two equations and solving for M yields:

$$M \equiv \begin{pmatrix} a'_x & b'_x \\ a'_y & b'_y \end{pmatrix}^{-1}. \quad (18)$$

Note that the resulting linear transformation will exist as long the matrix formed by \mathbf{a}' and \mathbf{b}' is invertible, that is, if both vectors are linearly independent. This condition is met by any non-degenerate parallelogram.

The new domain is a square of unit side, defined by the vertex

$$\mathbf{OP}^* = \begin{pmatrix} x_P^* \\ y_P^* \end{pmatrix} \equiv M \mathbf{OP}, \quad (19)$$

and side vectors $\mathbf{a}'^* = (a'_x, a'_y) \equiv (1, 0)$ and $\mathbf{b}'^* = (b'_x, b'_y) \equiv (0, 1)$. The covariance matrix will transform to:

$$\begin{pmatrix} \sigma_x^{*2} & \sigma_{xy}^* \\ \sigma_{xy}^* & \sigma_y^{*2} \end{pmatrix} \equiv M \begin{pmatrix} \sigma_x^2 & \sigma_{xy} \\ \sigma_{xy} & \sigma_y^2 \end{pmatrix} M^T, \quad (20)$$

which is in general not diagonal.

In the algorithm by Genz a correlation matrix instead of a covariance matrix is used, so one final transformation is needed. By applying two dilations (or contractions) of magnitudes $1/\sigma_x^*$ and $1/\sigma_y^*$ along the x and y axes, respectively, the

covariance matrix becomes a correlation matrix:

$$\begin{pmatrix} 1 & \rho' \\ \rho' & 1 \end{pmatrix} \equiv \begin{pmatrix} 1 & \sigma_{xy}^*/\sigma_x^*\sigma_y^* \\ \sigma_{xy}^*/\sigma_x^*\sigma_y^* & 1 \end{pmatrix}, \quad (21)$$

and the domain becomes a rectangle of vertex

$$\mathbf{OP}^{**} = \begin{pmatrix} x_0^*/\sigma_x^* \\ y_0^*/\sigma_y^* \end{pmatrix}, \quad (22)$$

and side vectors $\mathbf{a}'^{**} = (a_x'^{**}, a_y'^{**}) = (1/\sigma_x^*, 0)$ and $\mathbf{b}'^{**} = (b_x'^{**}, b_y'^{**}) = (0, 1/\sigma_y^*)$.

Calling *Rect* the new domain, it is possible to write

$$\begin{aligned} & \frac{1}{2\pi\sigma_x\sigma_y} \int_{Par} dx dy \exp -\frac{1}{2} \left(\frac{x^2}{\sigma_x^2} + \frac{y^2}{\sigma_y^2} \right) = \\ & \frac{1}{2\pi\sqrt{1-\rho'^2}} \int_{Rect} dx dy \exp \frac{-(x^2 - 2\rho'xy - y^2)}{2(1-\rho'^2)} = \\ & \Phi(Rect, \rho'), \end{aligned} \quad (23)$$

where the latter can be computed numerically by combining four calls to the bivariate normal probability function considered by Genz:

$$\begin{aligned} & \Phi(Rect, \rho') = \\ & L(x'_0, y'_0, \rho') - L(x'_0 + a'_x, y'_0, \rho') - \\ & L(x'_0, y'_0 + b'_y, \rho') + L(x'_0 + a'_x, y'_0 + b'_y, \rho'). \end{aligned} \quad (24)$$

We have programmed a web app implementing $\Phi(Rect, \rho')$ in JavaScript, which can be found (together with its source code) at <http://sdg.aero.upm.es/index.php/online-apps/gaussian-over-parallelogram>.

4 Example

Let $\mathbf{OP} = (0, 0, 0)$, $a = 2$, $b = 1$, $c = 3$, $\theta_a = \pi/4$, $\theta_b = \pi/3$, $\varphi_a = 0$ and $\Sigma = \begin{pmatrix} \sigma_x^2 & \sigma_{xy} \\ \sigma_{xy} & \sigma_y^2 \end{pmatrix} = \begin{pmatrix} 100 & 0 \\ 0 & 100 \end{pmatrix}$. Then the corners of the parallelograms are found using formula 14. The parallelograms are depicted in the figure. For the parallelograms (a, b) , (b, c) and (c, a) their coordinates are, respectively:

$$\{(0., 0.), (1.41421, 0.), (0.914214, 0.707107), (-0.5, 0.707107)\},$$

$$\{(0., 0.), (-1.5, -2.12132), (-2., -1.41421), (-0.5, 0.707107)\}$$

and

$$\{(0., 0.), (1.41421, 0.), (-0.0857864, -2.12132), (-1.5, -2.121329)\}.$$

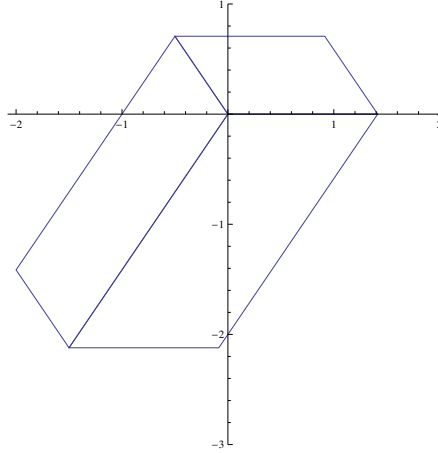


Fig. 5 The parallelograms are the projections of the faces of the rectangular cuboid onto the collision plane.

The coordinates of the corners of each parallelogram can be introduced in the app to yield the following result for the parallelograms (a, b) , (b, c) and (c, a) , respectively: $0.000015... + 0.000033... + 0.000047... \approx 0.000097$.

5 Future developments

We have assumed here that the attitude of the rectangular cuboid is known and fixed. However, its attitude could be changed without changing the projection of its center of mass. This does not have in general a dramatic effect on the probability of collision, but when the probability of collision is a little above the allowed threshold a change of attitude could bring it below the threshold, especially when the cuboid departs significantly from a cube. When the rectangular cuboid is a cube the ratio of the largest projected area to the smallest projected area is already $\sqrt{3} \approx 1.73$ and it is larger for any other rectangular cuboid. In the case of a cube the smallest projected area happens when the collision plane is parallel to some face of the cube; the largest projected area happens when the collision plane is perpendicular to a straight line joining opposite vertices of the cube. In the latter case the projection of the cube is a regular hexagon. We believe that the most advantageous attitude to avoid a collision is when the projection of the rectangular cuboid is the smallest face with its longest side tangent to some line of equal probability.

The most important generalization of this work is to extend it to the case of debris whose size is not negligible compared to the spacecraft. We plan to do this along the lines suggested by reference [9].

Last, a similar study could be carried out for spacecraft of shape a general cuboid, that is, a parallelepiped. But this case is rare.

6 Conclusions

An efficient and straightforward method for the evaluation of the collision probability between a rectangular cuboid and a small debris has been presented, leveraging the fact that the planar projection of the cuboid on the collision plane can be decomposed as three parallelograms. The collision probability for each parallelogram has been computed following the approach proposed by the authors in a recent work, by applying a linear transformation to change the domain into a rectangular one and using a numerical algorithm for the evaluation of bivariate normal probability distributions. This solution improves on the enveloping sphere approximation by retaining the parallelepiped shape of the first object, which better approximate common satellite geometries and other elements such as solar arrays. The high computational efficiency of the method is highlighted by the availability of a web-based sample implementation. Finally, a representative numerical example has been provided.

Acknowledgements This work has been supported by the ESA Contract No. 4000119560/17/F/MOS ('Environmental aspects of passive de-orbiting devices'). This work has been supported by the Spanish Ministry of Economy and Competitiveness within the framework of the research project ESP2017-87271-P

Appendix

Let us consider the following bivariate normal (BVN) probability:

$$L(h, b, \rho) = \frac{1}{2\pi\sqrt{1-\rho^2}} \int_h^\infty \int_k^\infty \exp\left(-\frac{x^2 - 2\rho xy + y^2}{2(1-\rho^2)}\right) dx dy \quad (25)$$

related to the standard BVN distribution as $\Phi((x_0, y_0), \rho) = L(-x_0, -y_0, \rho)$. Although it would be possible to evaluate Eq. 25 directly using a 2D numerical integration method, a faster algorithm can be achieved by reducing the problem to a single integral. Following previous work by Drezner and Wesolowski [7], Genz proposed in [11] to apply the formula for the partial derivative of the BVN distribution with respect to the correlation derived by Plackett [13]:

$$\frac{\partial L(h, k, r)}{\partial r} = \frac{1}{2\pi\sqrt{1-r^2}} \exp \frac{-(h^2 - 2rhk + k^2)}{2(1-r^2)}, \quad (26)$$

and integrate it over r to obtain an expression for L in terms of a single integral in the correlation.

The most straightforward choice would be to integrate between 0 and ρ , since the initial value for L at $r = 0$ is easily computed as the product of two univariate normal distributions. However, the singularity at $|r| = 1$ harms the accuracy of the numerical integration for cases with $|\rho| \sim 1$. To alleviate this issue Drezner and Wesolowsky [7] proposed to integrate instead between ρ and $\text{sign}(\rho)$: integrating only over the small region close to the singularity improves the numerical behavior, and the value of L at $r = \pm 1$ can also be expressed in terms of univariate normal distributions. Unfortunately, this new integral can still present numerical problems for h close but not equal to $\text{sign}(\rho)k$. Drezner and Wesolowsky circumvented this by applying a clever trick: they expanded part of the integrand in Taylor series of $\sqrt{1-r^2}$, providing the analytic integral of the polynomial part and performing the numerical integral of the remainder. The original work by Drezner and Wesolowsky [7] uses the Taylor expansion up to order 3, and Genz [11] later extended the result to order 5.

Building upon all these developments, Genz [11] defined an efficient algorithm for the numerical evaluation of L in double precision. On the one hand, he used the integral between 0 and ρ for $|\rho| \leq 0.925$, and the modified integral between ρ and $\text{sign}(\rho)$ for $|\rho| > 0.925$. To improve the numerical treatment of the integrands, he did the changes of variable $r = \sin(\theta)$ and $x = \sqrt{1-r^2}$, respectively. On the other hand, he applied Gauss-Legendre integration rules with enough points to maintain an absolute error less than $5 \cdot 10^{-16}$ (following extensive numerical tests, he proposed the 6 points rule for $|\rho| < 0.3$, the 12 points rule for $0.3 \leq |\rho| < 0.75$, and the 20 points rule for $|\rho| > 0.75$). We have used an in-house implementation of the original Genz algorithm, modified in order to deal with the more general problem of integrating the Gaussian over a parallelogram.

References

1. Akella, M.R., Alfriend, K.T.: Probability of collision between space objects. *Journal of Guidance, Control, and Dynamics* **23**(5), 769–772 (2000). doi: 10.2514/2.4611
2. Alfano, S.: A numerical implementation of spherical object collision probability. *Journal of the Astronautical Sciences* **53**(1), 103–109 (2005)
3. Bombardelli, C., Hernando-Ayuso, J.: Optimal impulsive collision avoidance in low earth orbit. *Journal of Guidance, Control, and Dynamics* **38**(2), 217–225 (2015). doi: 10.2514/1.G000742
4. Castellet, M., Llerena, I.: *Álgebra lineal y geometría*. Reverté (1992). ISBN: 978-8429150094
5. Chan, F.K.: *Spacecraft Collision Probability*. American Institute of Aeronautics and Astronautics (2008). ISBN-13: 978-1884989186, doi: 10.2514/4.989186.
6. Coppola, V.T.: Including velocity uncertainty in the probability of collision between space objects. In: *AAS/AIAA Spaceflight Mechanics Meeting* (2012). AAS 12-247

7. Drezner, Z., Wesolowsky, G.O.: On the computation of the bivariate normal integral. *Journal of Statistical Computation and Simulation* **35**(1-2), 101–107 (1990). doi: 10.1080/00949659008811236
8. Foster, J.L., Estes., H.S.: A parametric analysis of orbital debris collision probability and maneuver rate for space vehicles. NASA/JSC-25898 (1992)
9. García-Pelayo, R., Gonzalo, J.L., Bombardelli, C.: Rate and collision probability of tethers and sails against debris or spacecraft. *Journal of Guidance, Control, and Dynamics* **in press**, 1–13 (2019)
10. García-Pelayo, R., Hernando-Ayuso, J.: Series for collision probability in short-encounter model. *Journal of Guidance, Control, and Dynamics* **39**(8), 1908–1916 (2016). doi: 10.2514/1.G001754
11. Genz, A.: Numerical computation of rectangular bivariate and trivariate normal and t probabilities. *Statistics and Computing* **14**(3), 251–260 (2004). doi: 10.1023/B:STCO.0000035304.20635.31
12. Patera, R.P.: General method for calculating satellite collision probability. *Journal of Guidance, Control, and Dynamics* **24**(4), 716–722 (2001). doi: 10.2514/2.4771
13. Plackett, R.L.: A reduction formula for normal multivariate integrals. *Biometrika* **41**(3/4), 351–360 (1954). doi: 10.2307/2332716
14. Serra, R., Arzelier, D., Joldes, M., Lasserre, J.B., Rondepierre, A., Salvy, B.: Fast and accurate computation of orbital collision probability for short-term encounters. *Journal of Guidance, Control and Dynamics* **39**(5), 1009–1021 (2016). doi: 10.2514/1.G001353